Study of jets from rectangular nozzles with square grooves

P. Arun Kumar
arunkumr@iitk.ac.in

S. B. Verma and S. Elangovan
Experimental Aerodynamics Division
National Aerospace Laboratories-CSIR
Bangalore, India

ABSTRACT

An experimental study has been carried out to understand jet flow development from plain and grooved rectangular nozzles of aspect ratio 2:1 using two-component hotwire anemometry. Grooves of square configuration (side 4mm) and length 5mm were introduced in the (i) minor-axis, (ii) major-axis and, (iii) in both minor- and major-axes directions. The equivalent diameter of the plain rectangular nozzle is 37·5mm. Studies were carried out for a nominal jet exit velocity of 20ms^{-1} and for Reynolds number based on equivalent diameter of 54,000. The introduction of grooves in either plane does not show any influence on the potential-core length but results in faster jet-decay thereafter. It is observed that the grooves when introduced in minor-axis direction inhibit the jet growth in that plane while promoting the jet growth along major-axis plane and hence, delays the phenomena of axis-switching. However when introduced in major-axis direction, the grooves promote jet growth along major-axis plane while inhibiting jet-growth in minor-axis plane. Cross-sectional contours of mean-velocity suggest that the grooves modify the process of overall jet development significantly in the plane in which they are introduced relative to the plain jet and hence, significantly affect the axis-switching location in each case.

NOMENCLATURE

s	side of square groove, mm
D_e	equivalent diameter of rectangular exit, mm
l	length of square groove, mm
m_{exit}	mass flow rate at the nozzle exit
m_j	mass flow rate at any axial location along the jet centerline
U_e	mean velocity at nozzle exit, ms^{-1}
U	local mean velocity, ms^{-1}
K_u	mean streamwise velocity decay rate,
C_u	kinematic virtual origin (end of the potential core length non dimensionalised by the nozzle equivalent diameter)
u'/U_e	non-dimensional velocity fluctuation along X-direction
v'/U_e	non-dimensional velocity fluctuation along Y-direction
X	co-ordinate along the jet axis, mm
Y	co-ordinate along the horizontal plane, mm
$Y_{0.5}$	jet half-width along Y axis, mm
Z	co-ordinate along the vertical plane, mm
$Z_{0.5}$	jet half-width along Z axis, mm

Paper No. 3593. Manuscript received 8 June 2010, revised version received 21 September, 2010 accepted 3 December 2010.
This is the latest in a series of invited survey papers focusing on a specific aspect of the aeronautical industry.

https://doi.org/10.1017/S0001924000005583 Published online by Cambridge University Press

1.0 INTRODUCTION

Jets issuing from non-circular nozzle geometries provide an efficient technique for passive flow control and have been the topic of extensive research[1]. Various mixing techniques have been investigated in literature. Jet characteristics, in general, are known to be closely related to the dynamics of shear flow originating at the nozzle exit, and hence are strongly affected by the shape of the nozzle from which they issue. As a result, frequently the jet geometry is dictated by the nature of application.

The most popular approach has been the use of non-circular nozzle exit geometries. Hsia *et al*[2] conducted experiments on jets from rectangular nozzles from incompressible to compressible flow regimes and found that saddle shape curve was found to appear for Mach number of 0·3in the mean velocity profiles along the major axis side for nozzle aspect-ratio of 50:3. This shape was found to get less pronounced as the Mach number was increased to 0·5 and 0·8. Rectangular jets[3] combine the aspect ratio (AR) features of an elliptic jet with the corner (vertex) features of square jets. Nozzle size shape, AR, initial turbulence level, and Reynolds number effect the development of the jet. These non-circular jets has been observed to undergo a three-dimensional deformation process associated with the azimuthal distortion and bending of the vortex ring wherein ambient mass is brought in towards the jet-centreline along the major-axis side, and jet mass is thrown out along the minor-axis side. This non-uniform self-induction process results in enhanced mixing between the jet and the ambient irrotational mass[3-6]. As a result, the jet undergoes an axis-switching phenomenon wherein it entrains more fluid and spreads faster in the minor-axis plane while it shrinks along the major-axis side.

Detailed experiments on elliptic jets have been carried out by Hussain and Husain[4] for aspect-ratios in the range of 2:1 to 8:1. It was observed that for a given equivalent diameter, the aspect-ratio is an important parameter controlling the deformation and typological changes, that is, bifurcation of large-scale vortical structures in elliptic jets, and that the dynamics of low aspect-ratio elliptic jet are basically different from that of jets of moderate aspect-ratios. In addition, the axis-switching location was found to be linear function of aspect-ratio in elliptic and rectangular jets for the entire range of aspect-ratios studied. Non axisymmetric or the three-dimensional jets have been found to spread and mix faster than axisymmetric jets. Ho and Gutmark[5] investigated flow characteristics of an elliptic jet with an aspect ratio of 2:1. The mass entrainment before the end of the potential core was found to be three to eight times higher than that in an axisymmetric or a two dimensional jet. Experimental study of the influence of aspect-ratio on turbulent free jet flows from sharp-edged rectangular slots was investigated by Quinn[6] for aspect ratios of 2, 5, 10, 20 and found that the speed of mixing in the very near flow field (X/D_e < 5) increases with increase in aspect-ratio. Indeed, in the region the highest shear-layer values of the turbulent kinetic energy, the Reynolds shear stress and the turbulent transport of the Reynolds stresses are found in the aspect-ratio 20 jet, which also has the shortest potential core. Krothapalli *et al*[1] characterised the rectangular jet flow by three distinct regions when the decay of the square of the axial mean velocity along the jet is used to describe the flow field. The mean velocity and the shear stress profiles show similarity about 30 widths (smaller dimension) downstream from the nozzle exit. The half width of jet varies linearly with downstream distance, with different slopes for different aspect-ratios and initial geometries. The rms velocity profiles show similarity in the second region but not in third region. For X/D_e less than 60, the profiles of axial mean velocity exhibit a saddle shape, while the profiles in region three approach the similarity profile of an axisymmetric jet. The rms velocity and the shear stress profiles, however, do not exhibit similarity for these downstream locations.

Experiments on turbulent free jet issuing from rectangular exits having different geometries and different aspect ratios[7] have shown that the growth and decay of the spanwise saddle-backed profile for temperature and streamwise turbulent intensity distribution shows a remarkable change according to aspect-ratio, exit shape and exit velocity. For jets issuing from orifices of w/h = 5, the peaks of the spanwise saddle-backed profile for velocity initially occur in the flow region near the corner of the exit. It is postulated that the peak is due to a mixing-retarded region. Marsters[8] presented that the saddle-backed velocity profiles that are related to the upstream shaping of nozzle was found in turbulent jet flows from a rectangular nozzles. These velocity peaks are as much as 20% greater than the centreline velocity. The peaks appear to merge downstream. Turbulent measurement indicates straight forward behaviour in the

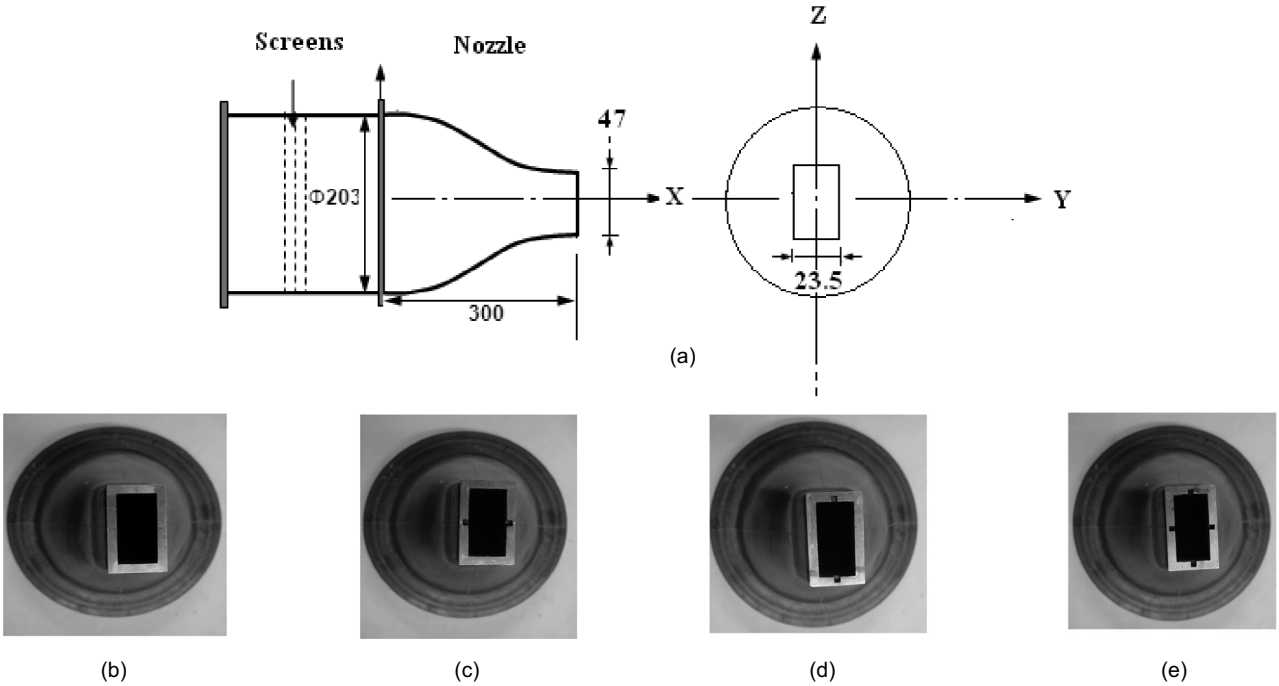


Figure 1(a). Schematic of the jet facility; Photos of the models (nozzle attachments) fabricated; (b) Plain attachment, (c) with grooves introduced in minor-axis direction, (d) with grooves introduced in major-axis direction and,(e) with grooves in both axes direction.

https://doi.org/10.1017/S0001924000005583 Published online by Cambridge University Press

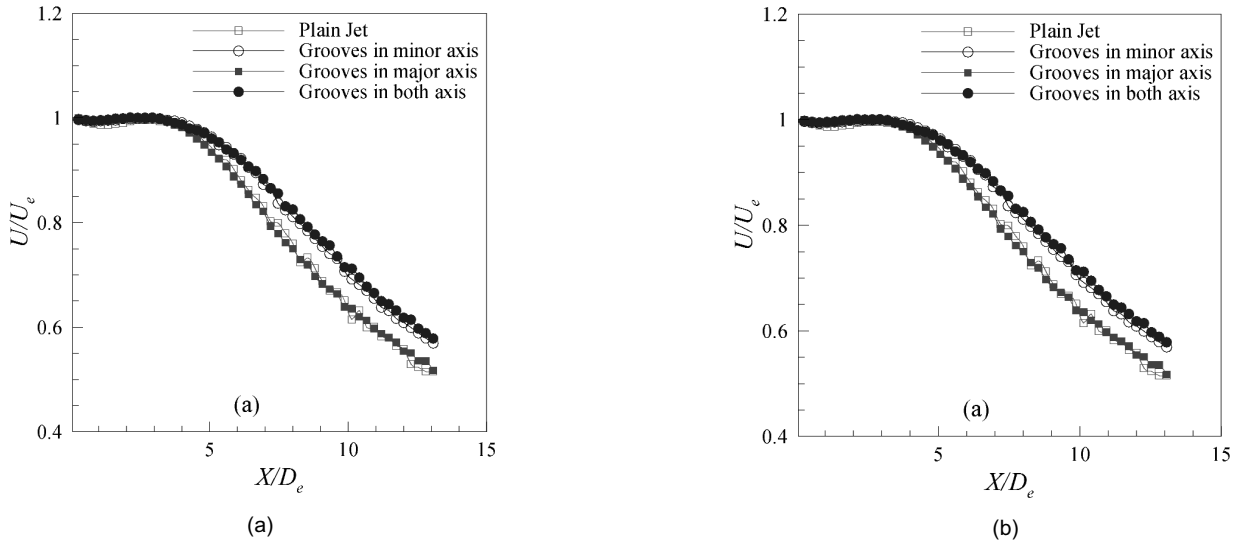


Figure 2. Comparison of centreline decay for (a) mean velocity and, (b) turbulent intensity.

shear layer on the long sides of the jets. Near the ends of the jets, however, the intensity of turbulence is much increased as the two shear layers growing on the jet ends and side interact. The velocity peaks which appear near the end of the jets cannot be explained in terms of the turbulence stresses alone. There is no mechanism in the normal and shearing stresses to account for the peak. Mi *et al*[9] stated that rectangular turbulent jet with sufficiently high aspect-ratio (> 15) is found to undergo in succession the following three distinct regions, initial quasi-plane-jet zone, transition zone, and final quasi-axisymmetric-jet zone. The jet may be treated approximately as a plane jet as long as it is in the first zone. The axial extend of the first zone increases with increase in aspect ratio. The normalised properties, such as mean velocity profiles and rms velocity profiles in this zone show only slight disparity, based on their evolution against x/h, for different aspect-ratios

The effects of internal grooves in high-speed circular jets were studied for the first time by Elangovan and Rathakrishnan[10] . These grooves were observed to improve the jet growth in the plane in which they are introduced thereby weakening the shock-cell structure relative to plain circular jet. The effect of grooves cut along the inner surface of the diverging portion of a Mach 1·8 converging-diverging nozzle[11] were also observed to act as a effective passive control device resulting in enhanced jet-mixing and jet noise reduction. Most of the previous studies using grooves were made in circular jets. The objective of the present study was therefore to investigate the effect of grooves on jets issuing from rectangular nozzles. The presence of these grooves is observed to significantly modify the overall jet development. Further the effect of the presence of grooves in minor-axis and major-axis direction is also investigated.

2.0 EXPERIMENTAL SETUP AND PROCEDURE

Experiments were carried out in the low-speed jet facility (Fig. 1(a)) to investigate the near-field jet flow development from a 2:1 rectangular nozzle. The facility is driven by a fan-motor and has a settling chamber with three screens for flow quality treatment. The nozzle has a circular section of 203mm diameter, smoothly contoured to a 2:1 rectangular section ($2a$ = 47 ± 0·1mm and $2b$ = 23·5 ± 0·1mm) over a length of 300 ± 0·1mm, where $2a$ and $2b$ are major and minor-axis diameters, respectively. The equivalent diameter (D_e) of the rectangular nozzle is 37·5 ± 0·1mm and is defined as the diameter of a circular jet with nozzle exit area equivalent to that of a non-circular nozzle exit configuration. Grooves of square configuration (side 4 ± 0·1mm) and length 5 ± 0·1mm were introduced in the (i) minor-axis direction (Fig. 1(c)), (ii) major-axis direction (Fig. 1(d)) and, (iii) in both minor- and major-axes direction (Fig. 1(e)). Extensive hotwire measurements are carried out at a nominal jet exit velocity (Ue) of 20 ± 0·5ms^{-1} and the Reynolds number based on the equivalent diameter of the jet (D_e) is 5·4 ± 0·05 × 10^4. Measurements were carried out up to $13D_e$. The possible sources of errors in our present investigations are due to the movement of traverse along X, Y and Z-directions, setting the exit velocity for measurements, the possible inaccuracies in nozzle dimensions. Positioning accuracy is ±0·1mm in the X, Y and Z-directions, and the velocity at the exit of the rectangular nozzle was maintained with 20 ± 0·5ms^{-1} for the experiments.

Hotwire measurements were carried out at several axial locations by means of a 99N10 DANTEC anemometry system using a Dantec 55P11 two-component probe. The hotwires were operated on a constant temperature with an overheat ratio of 1:5. The probe has platinum plated tungsten wires (1·25mm long and 5µm diameter) and can be used for air applications with turbulent intensities up to 5–10. The X-wire was positioned in the flow in such a way that it allowed measurement of the fluctuations of streamwise velocity (u') and transverse velocity (v'). The positioning of the anemometer sensor was performed by using a PC-controlled precision positioning device. The probe was calibrated using Dantec 9054H01 calibrator with 120mm^2 nozzle in the velocity range between 0 and 25ms^{-1}. The signals from the probe were acquired at a sampling rate of 3kHz with 10,000 samples. The anemometer analog output was acquired by using a differential mode National Instruments PCI-6036E having 16-bit resolution, operating range of ±10V and maximum scan rate of 200Ks/samples. The linearisation and processing of the hotwire signal was then carried out digitally. The actual streamwise velocity U and the perpendicular velocity V were calculated from the hotwire anemometer output according to King's law equation and equation procedure by Jorgenson.

3.0 RESULTS AND DISCUSSIONS

3.1 Mean centreline velocity decay

Figure 2(a) shows the centreline velocity decay for the jets from plain and grooved nozzles. The local centreline velocity (U) is normalised by the exit velocity (U_e) and is plotted against the axial

https://doi.org/10.1017/S0001924000005583 Published online by Cambridge University Press

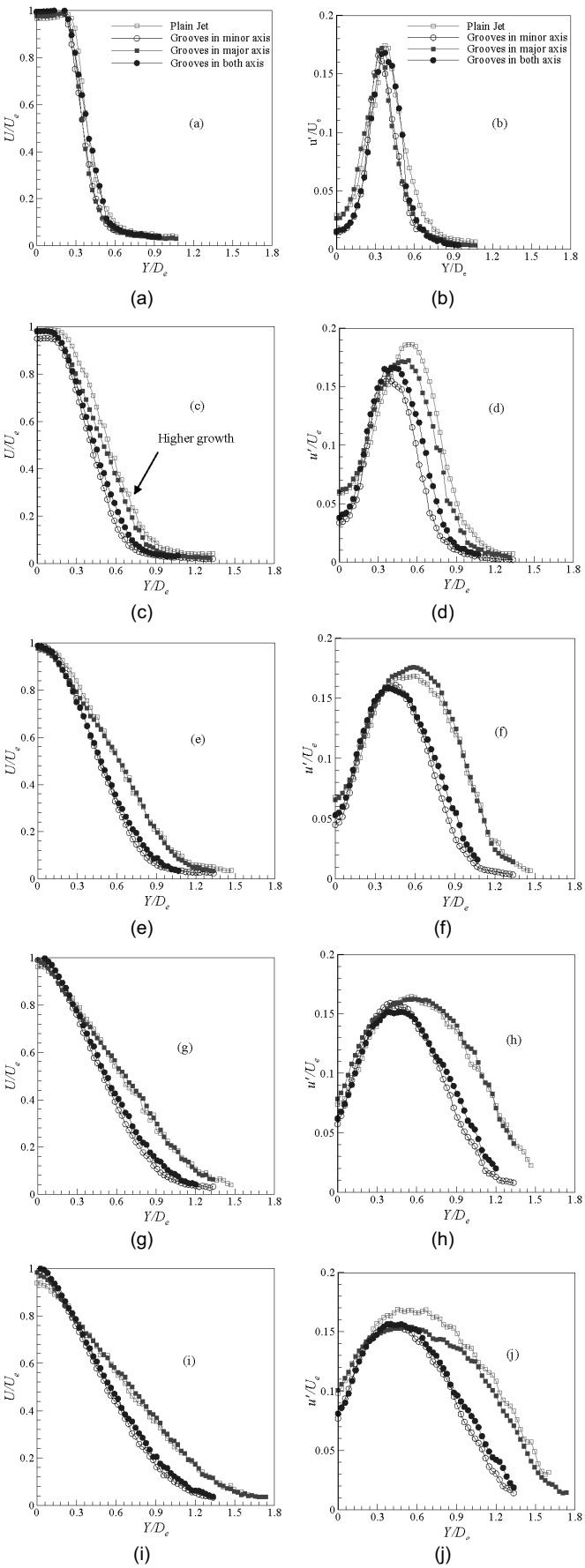


Figure 3. Mean velocity and the corresponding turbulence profiles along minor-axis side for; (a)-(b) X/D_e = 1·0, (c)-(d) X/D_e = 2·0, (e)-(f) X/D_e = 3·0, (g)-(h) X/D_e = 4·0, (i)-(j) X/D_e = 5·0.

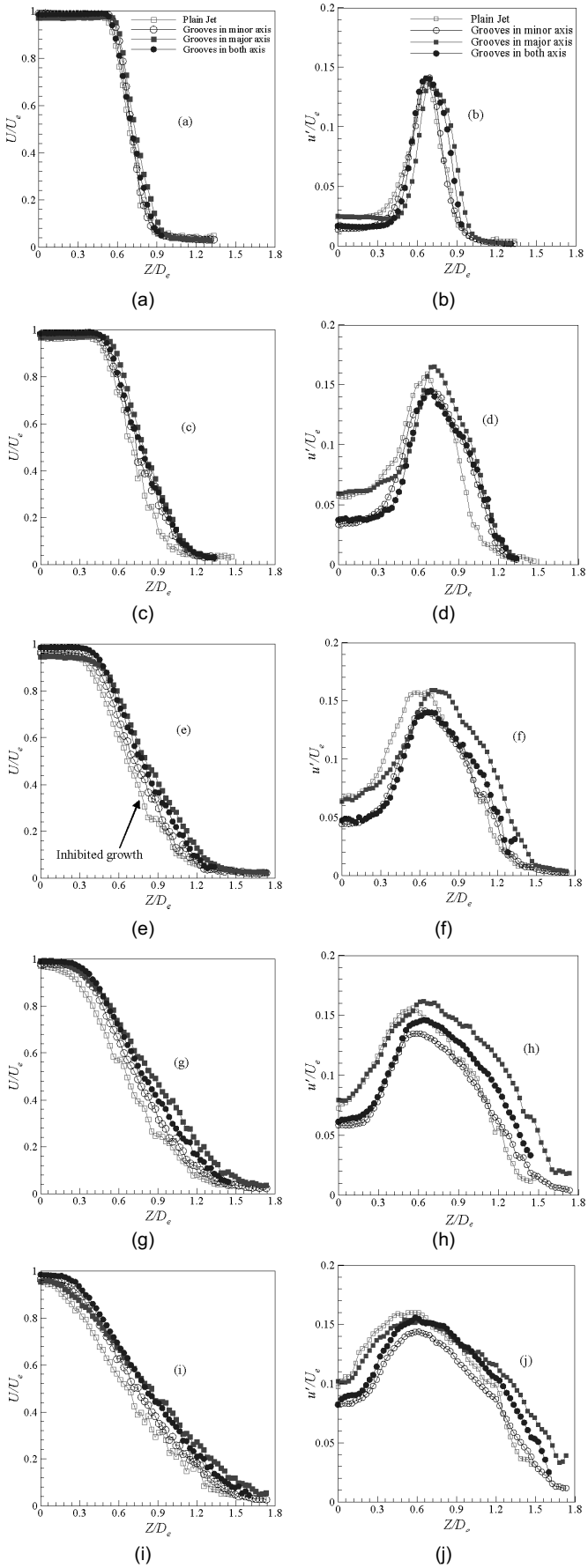


Figure 4. Mean velocity and the corresponding turbulence profiles along major-axis side for; (a)-(b) X/D_e = 1·0, (c)-(d) X/D_e = 2·0, (e)-(f) X/D_e = 3·0, (g)-(h) X/D_e = 4·0, (i)-(j) X/D_e = 5·0.

https://doi.org/10.1017/S0001924000005583 Published online by Cambridge University Press

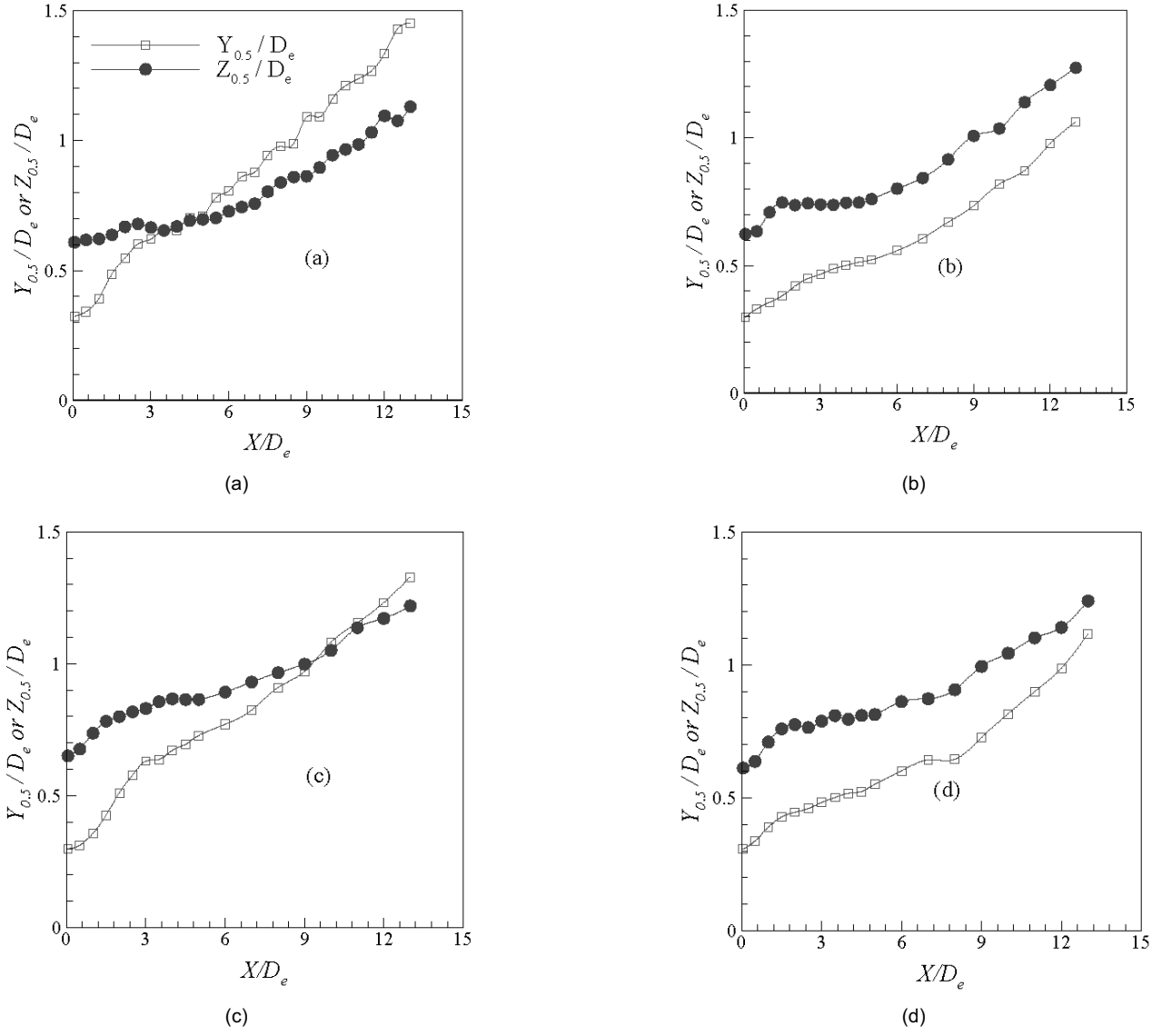


Figure 5. (a) Jet half-width growth for (a) plain jet, (b) jet with grooves in minor axis direction, (c) jet with grooves in major-axis direction, (d) jet with grooves in both axes direction.

distance normalised by the nozzle equivalent diameter (D_e). It is observed that the potential core-length extends up to X/D_e of 3·73 for the plain jet and for the jet with grooves in major-axis direction. However for jets with grooves in minor-axis direction and in both axes, the potential core-length extends up to X/D_e of 4. A linear regression analysis was conducted in the range $X/D_e \geq 4$ up to X/D_e = 13 for the centreline decay behaviour using the formula[12].

$$U/U_e = K_u\,(X/D_e + C_u)$$

The variation is linear for all cases but with different mean velocity decay rates for different cases. The centreline velocity decay rates is the maximum for plain jet (0·056), followed by grooves in major-axis (0·053), grooves in minor-axis (0·050) and finally for grooves in both axes (0·048). The presence of the grooves in minor-axis direction and grooves in both axes direction reduces mixing thereby decreasing jet centreline velocity decay (increase in potential core-length). This value is a minimum for plain jet and increases for grooves in major axis, grooves in minor axis, and for grooves in both axes. The value of K_u and C_u shows that the plain jet has better mixing and decay of mean centreline velocity, when compared with the other three exit configurations (grooved nozzles).

Figure 2(b) shows the variation of turbulence intensity along the axial distance. The centreline turbulence intensity (u'/U_e) increases and peaks in the region of maximum velocity decay. It is the lowest for the case of grooves in both axes followed by the case of grooves in minor-axis, grooves in major-axis, and finally shows the highest values for plain jet. The location of this peak along the axial distance varies from X/D_e of 7·5 to 8·5 for the above cases. Introducing grooves at the nozzle exit therefore not only reduces the peak value of turbulence intensity, but also shifts the peak location further downstream.

3.2 Mean velocity profiles

Figures 3(a)-(b) show a comparison of mean velocity (U/U_e) and the corresponding turbulence (u'/U_e) profiles along the minor-axis side for various nozzle exit configurations at X/D_e = 1·0. Relative to the plain jet, the nozzle with grooves in minor-axis direction shows an inhibited shear-layer growth and reduced turbulence level which becomes more apparent as the jet develops further downstream, Figs. 3 (c)-(j). For $X/D_e \geq 2{\cdot}0$, the shear-layer growth patterns become more distinct with the plain jet showing highest growth followed by jet with grooves in major-axis direction, grooves in both axes

https://doi.org/10.1017/S0001924000005583 Published online by Cambridge University Press

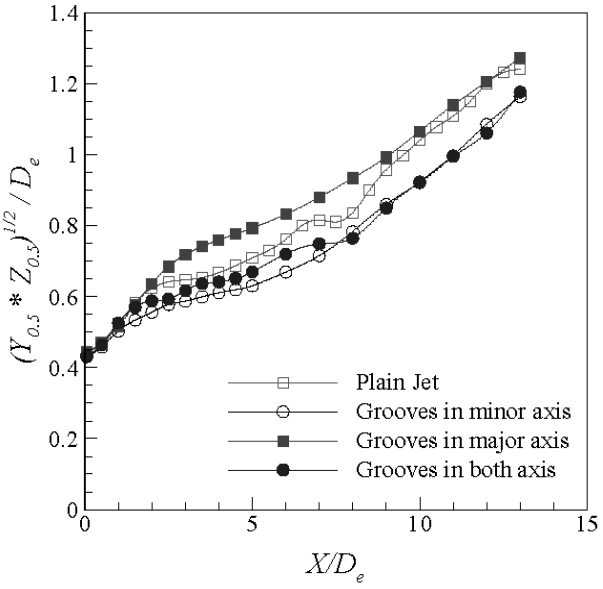


Figure 6. Comparison of the equivalent jet half width for all the test cases.

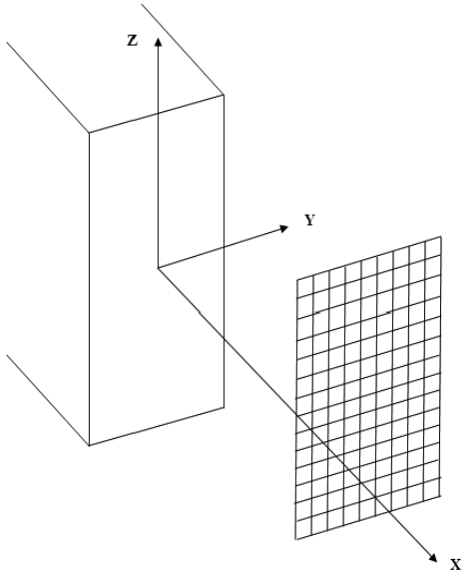


Figure 7. Grid measurement plane (*Y-Z*) for overall jet development.

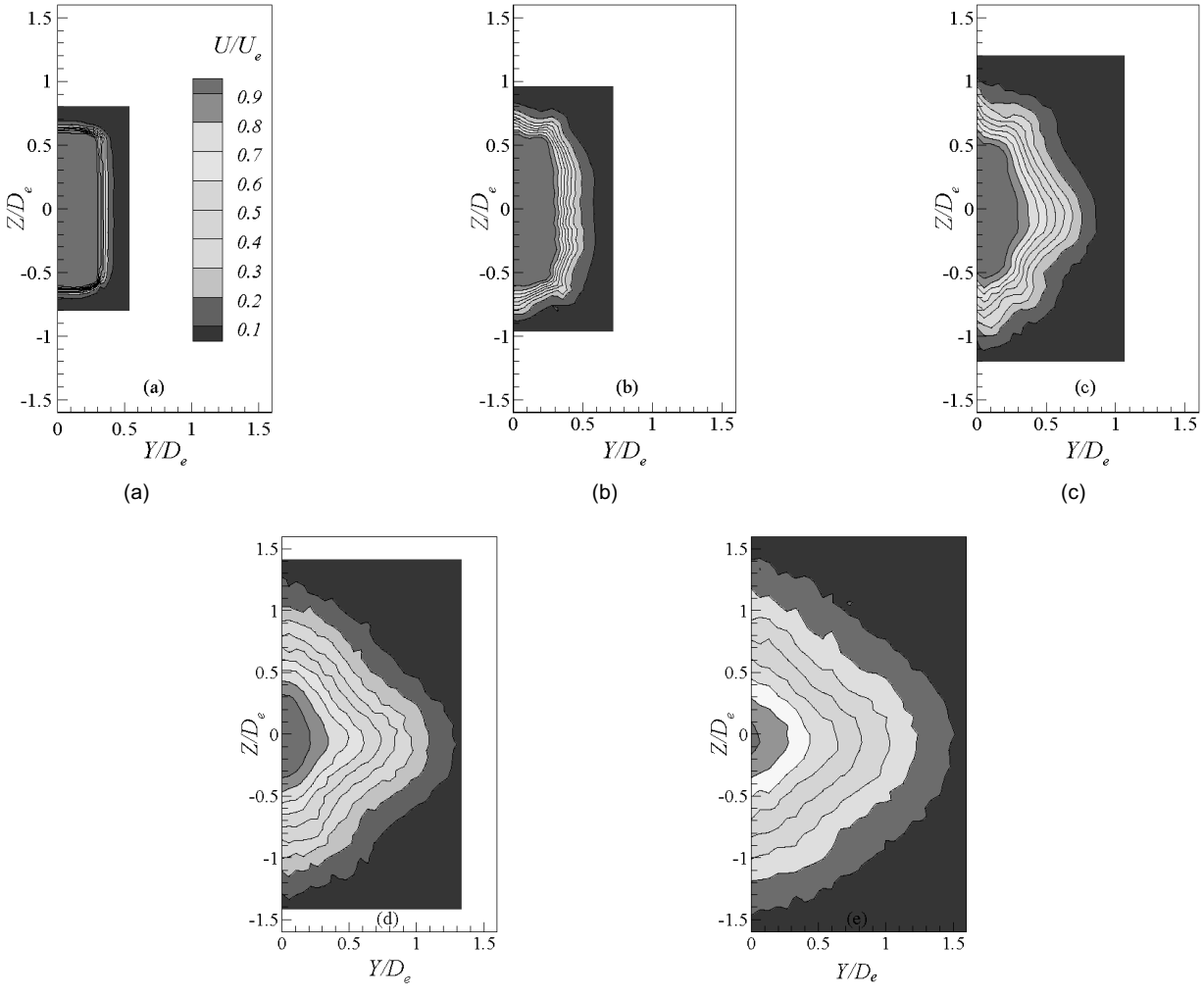


Figure 8. Mean velocity contour for plain rectangular jet; (a) X/D_e = 0·5, (b) X/D_e = 1·0, (c) X/D_e = 2·0, (d) X/D_e = 4·0, (e) X/D_e = 6·0.

https://doi.org/10.1017/S0001924000005583 Published online by Cambridge University Press

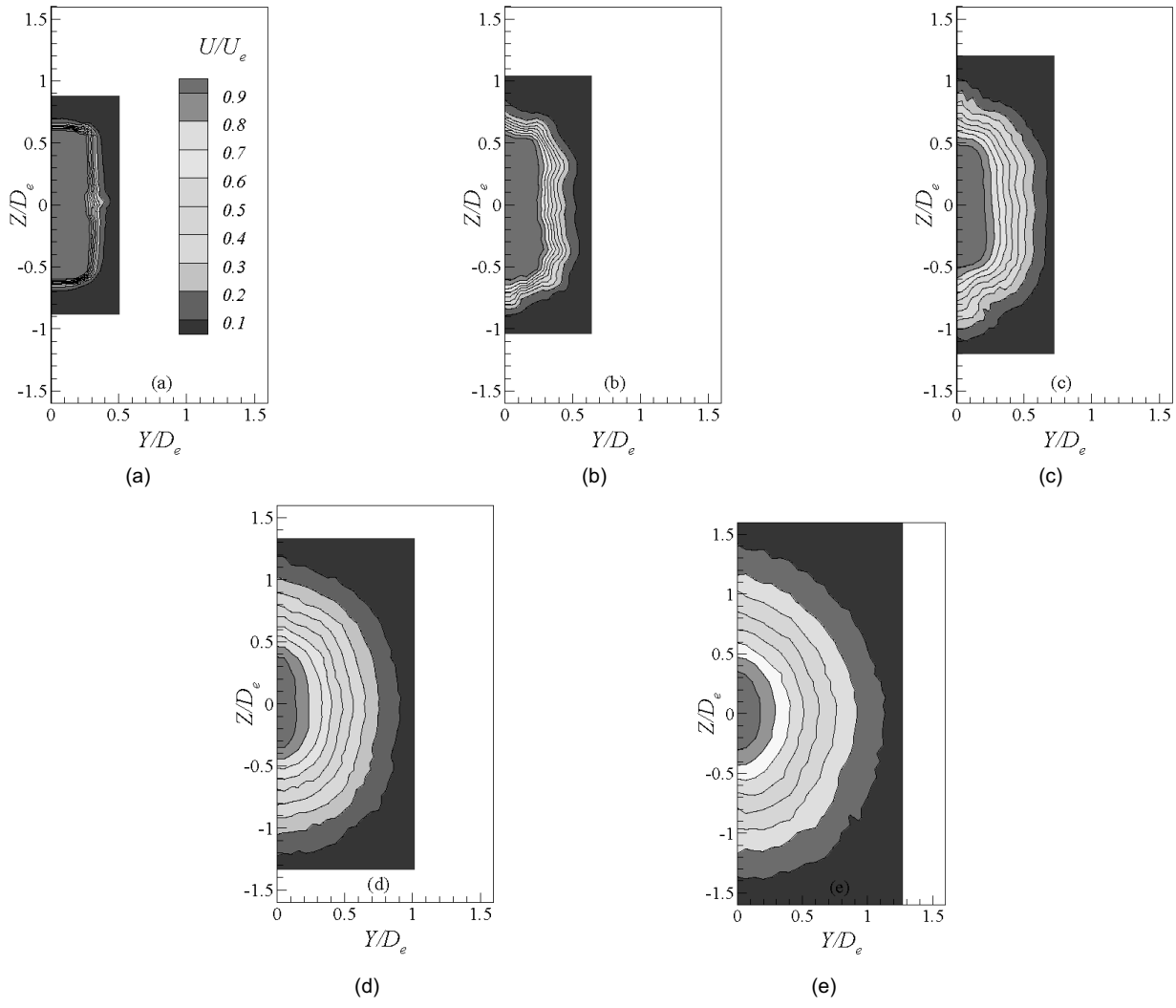


Figure 9. Mean velocity contour for grooves in minor-axis direction; (a) X/D_e = 0·5, (b) X/D_e = 1·0, (c) X/D_e = 2·0, (d) X/D_e = 4·0, (e) X/D_e = 6·0.

direction and finally, by jet with grooves in minor-axis direction. However, at X/D_e = 4·.0 and 5·0 as shown in Fig. 3(g)-(j), the plain jet and the jet with grooves in major axis show similar mixing characteristics while the jet with grooves in minor-axis direction and the jet with grooves in both-axis direction show similar growth patterns and with significantly reduced shear-layer growth.

Some interesting features can also be observed from the mean velocity (U/U_e) and the corresponding turbulence (u'/U_e) profiles along major-axis side, as shown in Fig. 4. Here it can be seen that the presence of grooves in major-axis direction shows a higher shear-layer growth, a feature completely opposite to that observed in jets with grooves in minor-axis direction. The shear-layer growth patterns, once again, become more distinct for $X/D_e \geq 2{\cdot}0$ where it is seen that the jet with grooves in major-axis direction shows highest growth followed by the jet with grooves in both axes direction, the jet with grooves in minor-axis direction and finally, by the plain jet. At X/D_e = 4·0 and 5·0, the jet with grooves in minor-axis and on both axes show similar mixing characteristics while the jet with grooves in major-axis direction shows higher growth relative to plain jet. The turbulence levels are seen to be the highest for the jet with grooves in major-axis direction followed by the plain jet, the jet with grooves in both axes direction and finally, by the jet with grooves in minor-axis direction.

The above results show that the introduction of grooves alters the growth characteristics of the nozzle plane in which they are introduced and hence, delays the axis-switching phenomenon in each case. The plain jet, on the other hand, shows the higher shear-layer growth along minor-axis side while it shows an inhibited growth along major-axis side which causes the jet to switch earlier that the jets issuing from grooves nozzles and is discussed in the next section.

3.3 Jet half-width growth

Figure 5 (a) shows the jet half-width growth in both planes for the plain jet. It can be clearly seen that the jet spreads rapidly along minor-axis and slower along major-axis plane for plain jet with the axis-switching occurring at X/D_e of 4·5. For the case of jet with grooves in minor-axis direction, the jet spreads slowly along minor axis relative to plain jet. Along major-axis this jet spreads faster when compared to the plain jet. This prevents axis-switching (Fig. 5(b)) in this case. For the case of jet with grooves in major-axis direction, the jet spread along the minor-axis is similar to that of plain jet but along the major axis the spread is faster when compared to plain jet. This delays the axis-switching and pushes the axis switchover location downstream. The crossover location for this case is X/D_e = 9·5 (Fig. 5(c)). For exit geometry with grooves in both axes direction, the jet spread along minor-axis is slower and resembles the trend similar to that of grooves in minor-axis direction, but the spread in major-axis is similar to that of grooves in major-axis direction and the spread is faster than plain jet. As such the axis-switching phenomena is further delayed and the location of crossover is X/D_e = 15 (Fig. 5(d)). It is seen that the presence of

https://doi.org/10.1017/S0001924000005583 Published online by Cambridge University Press

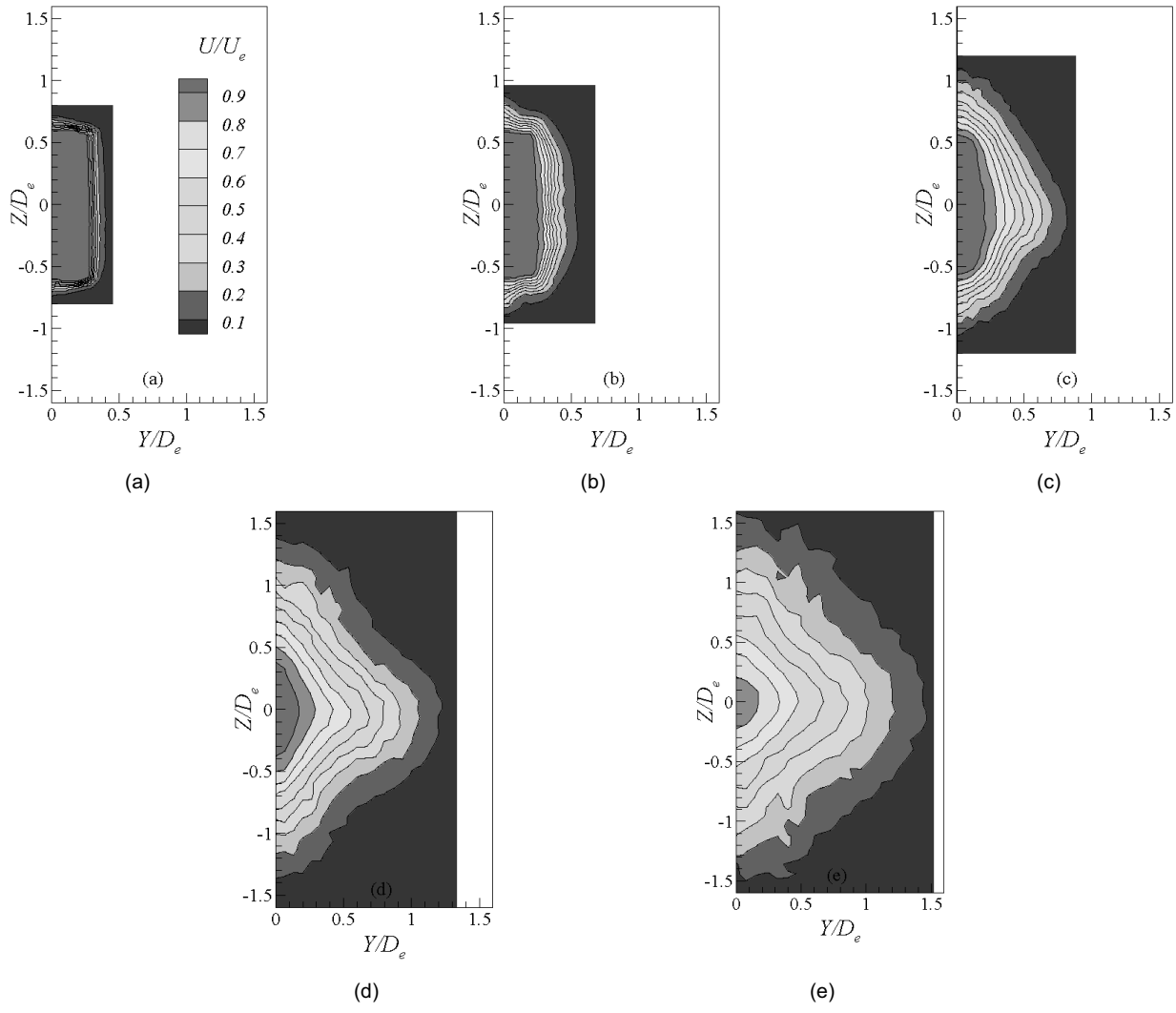


Figure 10. Mean velocity contour for grooves in major-axis direction; (a) X/D_e = 0·5, (b) X/D_e = 1·0, (c) X/D_e = 2·0, (d) X/D_e = 4·0, (e) X/D_e = 6·0.

grooves delays the axis-switching phenomena. This is because grooves when placed along minor-axis direction inhibit jet growth in that plane while they promote jet growth when introduced along the major axis direction.

3.4 Equivalent jet width

Although the jet width in each of the plane exhibits a nonlinear variation with axial distance for all case of the geometry, the equivalent jet width[12] shows a linear progression beyond $X/De \geq 5$. The equivalent jet spread signifies the overall spread of jet along the axial location for the exit condition. Figure 6 shows the equivalent jet spread non-dimensionalised by the equivalent diameter along the axial location. This depicts that the overall jet spread is more for the geometry with groove in major-axis direction and decreases via plain jet, grooves in both axes direction, and grooves in minor-axis direction. This shows that even though the plain jet switches axis earlier its overall jet development is lesser than the jet with grooves in major-axis direction.

3.5 Contours of mean velocity

Grid measurements were carried out at various axial locations to study the process of overall jet development. These measurements were made in one half of *Y-Z* plane of the jet (as shown in Fig. 7) with a step of $\Delta y = \Delta z = 1 \pm 0{\cdot}1$mm for X/D_e = 0·5 and 1, $\Delta y = \Delta z = 1{\cdot}5 \pm 0{\cdot}1$mm for X/D_e = 2, $\Delta y = \Delta z = 2 \pm 0{\cdot}1$mm for X/D_e = 4 and 6 comprising of points approximately from 1,200 – 1,600. Figures 7-10 show a comparison of corresponding contours of mean velocity for all test nozzles at various axial locations. The variation in each successive contour level is $0{\cdot}1U_e$. In these measurements, the orientation of the hotwire probe was such that the streamwise component of the velocity U (X-direction) and the vertical component W (Z-direction) were measured.

Immediately downstream of the nozzle exit, the plain jet is seen to retain its original rectangular nozzle and shows a thin mixing-layer as is evident from the closely spaced contours, Fig. 8(a). As the jet begins to deform due to non-uniform induction of velocity, mixing between the jet and the ambient mass is initiated while vortices are generated from the nozzle corners (seen as a outward bump in contours), Fig. 8(b). As a result the jet starts a pumping action wherein ambient mass is brought in towards the jet centreline along the major-axis side while jet mass is thrown out along the minor-axis side. Further downstream the mixing layer begins to thicken and the jet cross section begins to change its shape as is indicated by a higher growth along minor-axis side (Fig. 8(a) – 8(e)). The spacing between the contour levels is seen to increase with increase in downstream distance. Figure 8(d) and 8(e) clearly shows that jet axis-switching has already taken place as was observed in Fig. 5(a).

Placement of grooves in minor-axis direction significantly modifies the overall jet development characteristics, Fig. 9. Relative to the plain jet, at X/D_e = 0·5, the contours in the region of the groove show a small indent in the mixing layer that points inwards spanning

https://doi.org/10.1017/S0001924000005583 Published online by Cambridge University Press

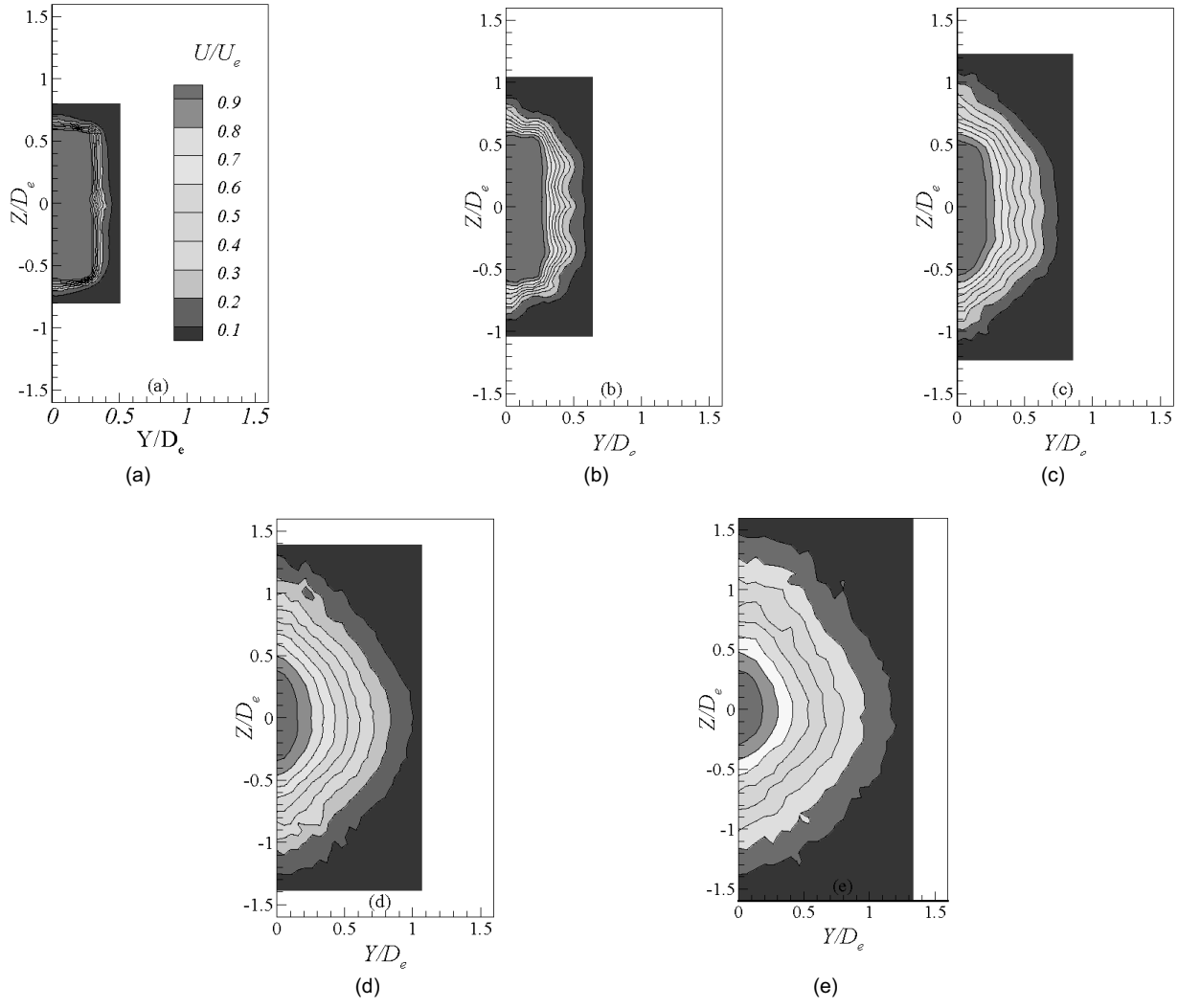


Figure 11. Mean velocity contour for grooves in both axes direction; (a) X/D_e = 0·5, (b) X/D_e = 1·0, (c) X/D_e = 2·0, (d) X/D_e = 4·0, (e) X/D_e = 6·0.

the width of the groove. At X/D_e = 1·0 this region shows an inhibited jet growth while the regions towards the corners continue to grow outwards as observed for plain jet, Fig. 9(a). Such a growth pattern is typical of a mushroom type flow structure which grows by bringing in high-speed fluid from the jet-core towards the groove base and inwards into the jet. Similar result of a sharp incursion of contours has earlier been reported for tabs which are known to generate streamwise vortices into the flow[13-17]. The net effect of such a structure is to inhibit jet growth in plane of groove placement while promoting growth along major-axis, as seen in Figs. 9(b) – 9(e). The jet cross-sectional shape at X/D_e = 6·0 looks elliptic in shape with no sign of a switch in jet axis. Although the present observation suggests the presence of streamwise vortices in the flow further detailed investigations need to be carried out to study the vortex dynamics from grooves.

On the other hand, placement of grooves in major-axis direction, however, results in an indentation that is directed outwards, Fig. 10. As a result, relative to plain jet, the jet grows faster along major-axis side while the minor-axis side grows similar to the plain jet. This is also seen to inhibit growth along the nozzle corners so that at X/D_e = 2·0, the jet shape takes the form of a rhombus which grows faster along both axis, Fig. 10(c). The higher jet growth along major-axis side delays the axis-switching phenomena which is still not observed to have occurred at X/D_e = 6·0, Fig. 10(e). Placement of grooves in both the axes direction shows inhibited jet growth along the minor-axis side while a higher jet growth is indicated along major-axis side, Fig. 11. This further delays the process of axis-switching phenomena.

The above results suggest that the groove generated structures play a significant role in modifying the jet growth in the plane in which they are introduced. This significantly affects the overall jet development and hence, the jet axis-switching location.

3.6 Mass entrainment

Induction of surrounding mass into the jet field by eddies at the jet periphery results in the jet mass entrainment. When this entrained fluid mass moves into the jet field, it acquires momentum from the jet flow and thereby reduces the momentum of the original fluid mass. The mass entrainment has a direct influence on the jet decay through the momentum exchange process. Therefore, higher the entrainment faster the decay will be.

Figure 12 shows the variation of the non-dimensionalised mass flow $(m_j\text{-}m_{exit})/m$exit along the axial distance (X/D_e) for the various test nozzles. Here the local mass flux (m_j) at different axial locations for different geometry was computed from the grid measurements in *Y-Z* plane and mexit is the mass at the nozzle exit at X/D_e = 0·5. It is observed that the mass entrainment is significantly large for the case of plain jet when compare to grooved nozzles. The mass entrainment almost shows a linear profile along the axial distance for all the cases. The mass entrainment is almost same for all geometries up to X/D_e of 1·0, and thereafter shows different values. This clearly shows

https://doi.org/10.1017/S0001924000005583 Published online by Cambridge University Press

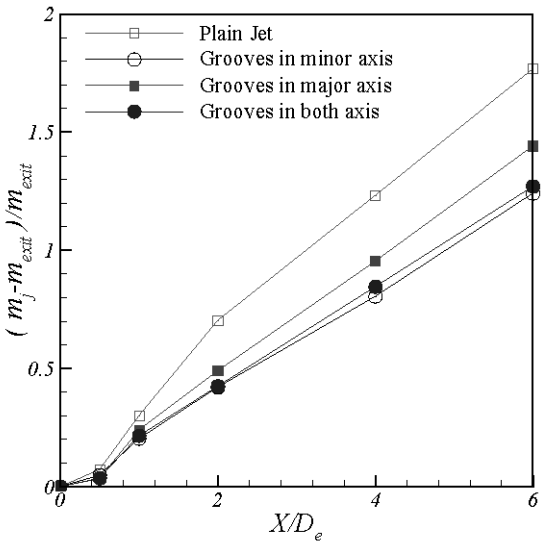


Figure 12. Comparison of mass entrainment for each test case.

that the presence of the grooves in the nozzle exit does not significantly influence the overall jet mixing characteristics. Application of such a configuration can be, perhaps, in impinging jets where suppression of mixing is desirable so as to ensure sufficient impact pressure on the surface.

4.0 CONCLUSIONS

An experimental investigation has been carried out to study the flow development from a jet issuing from a 2:1 rectangular nozzle with and without grooves using 2-component hotwire anemometer. Square grooves of side 4mm and length 5mm were separately introduced in the minor-axis direction, major-axis direction and on both axes direction of rectangular nozzle.

It is observed that grooves do not affect the length of the potential-core region but are seen to result in faster jet centreline decay thereafter when compared to plain jet. Contours of mean velocity reveal that when grooves are introduced in the minor-axis direction they inhibit jet growth in that plane whereas when introduced in major-axis direction, they promote jet growth in that plane. This significantly modifies the jet development phenomena in each test case and hence, delays the process of axis-switching relative to plain jet. The mass entrainment is however higher for the case of plain jet when compare to grooved nozzles. The presence of the grooves therefore does not significantly influence the overall jet mixing characteristics but influences the axis-switching phenomena considerably.

ACKNOWLEDGEMENT

The work reported here was carried out by the first author in the experimental aerodynamics division (EAD) at National Aerospace laboratories-CSIR, Bangalore, as a part of his M.E. Thesis work from MIT Chennai. The authors are thankful to Dr. A.R. Upadhya, Director, NAL, Bangalore for granting permission to work at NAL, and Dr. Sajeer Ahmed, Head EAD for carrying out the work in his division. Authors also express their sincere thanks to Mr. Sudhakar, Scientist EAD for his assistance in conducting the experiments.

REFERENCES

1. KROTHAPALLI, A., BAGANOFF, D. and KARAMCHETI, K. On the mixing of a rectangular jet, *J Fluid Mechanics*, 1981, **107**, pp 201-220.
2. HSIA, Y., KROTHAPALLI, A., BAGANOFF, D. and KARAMCHETI, K. Effects of Mach number on the development of a subsonic rectangular jet, *AIAA J*,1982, **21**, (2), pp 176-177.
3. GUTMARK, E.J. and GRINSTEIN, F.F. Flow control with non-circular jets, *Annual Review of Fluid Mechanics*, 1999, **31**, pp 239-272.
4. HUSSAIN, H.S. and HUSAIN, A.K.M.F. Elliptic jets part I: characteristics of unexcited and excited jets, *J Fluid Mechanics*, 1989, **208**, pp 257-319.
5. HO, C.M. and GUTMARK, E.J. Vortex induction and mass entrainment in a small-aspect ratio elliptic jet, *J Fluid Mechanics*, 1987, **179**, pp 383-405.
6. QUINN, W.R. On mixing in an elliptic turbulent free jet, *Physics of Fluids*, 1989, **10**, pp 1716-1721.
7. TSUCHIYA, Y., HORIKOSHI, C. and SATO, T. On the spread of rectangular jets, *Experiments in Fluids*, 1986, **4**, pp 197-204.
8. MARSTERS, G.F. Spanwise velocity distributions in jet from rectangular slots, *AIAA J*, **19**, (2), pp 148-152.
9. MI, J., DEO, R.C., and NATHAN, J. Characterization of turbulent jets from high-aspect-ratio rectangular nozzle, 2005, *Physics of Fluids*, **17**, pp 68102-1-68102-4.
10. ELANGOVAN, S. and RATHAKRISHNAN, E. Studies on high speed jets from nozzles with internal grooves, *Aeronaut J*, 2004, **108**, pp 43-50.
11. VISHNU, J. and RATHAKRISHNAN, E. Acoustic characteristics of supersonic jets from grooved nozzles, *J Propulsion and Power*, 2004, **20**, (3), pp 520-526.
12. SRINIVASAN, K. and RATHAKRISHNAN, E. Studies on polygonal slot jets, *AIAA J*, 1985, **38**, (10).
13. BRADBURY L.J.S. and KHADEM, A.H. The distortion of a jet by tabs, *J Fluid Mech*, 1975, **70**, pp 801–813.
14. CHUA, L.P., YU, S.C.M. and WANG, X.K. Flow visualization and measurements of a square jet with mixing tabs, *Exper Thermal Fluid Sci*, 2003, **27**, pp 731–744.
15. AHUJA, K.K. and BROWN, W.H. Shear flow control by mechanical tabs, AIAA paper 89-0094.
16. ZAMAN, K.B.M.Q., REEDER, M.F. and SAMIMY, M. Control of an axisymmetric jet using vortex generators, *Phys Fluids*, 1994, **6**, (2), pp 778–793.
17. VERMA, S.B., SUDHAKAR, S. and VENKATAKRISHNANA L. Experimental study on a jet issuing from an elliptic nozzle with cylindrical tabs, *J Turbulence*, 2010, **11**, 20, pp 1–24

https://doi.org/10.1017/S0001924000005583 Published online by Cambridge University Press